Electrical Potentials of Protoscoleces of the Cestode *Echinococcus granulosus* from Bovine Origin

Mónica P. A. Carabajal, Marcos A. Durán, Santiago Olivera,

María José Fernández Salom, and Horacio F. Cantiello

Laboratorio de Canales Iónicos, Instituto Multidisciplinario de Salud, Tecnología y Desarrollo (IMSaTeD, CONICET-UNSE), Santiago del Estero, 4206, Argentina

Running Title: *Electrical potentials of protoscoleces from Echinococcus granulosus*

***Corresponding author**:

Email: hcantiello@yahoo.com.ar

Abstract

Larval stages of the tenia *Echinococcus granulosus* are the infective forms of cystic echinococcosis or hydatidosis, a worldwide zoonosis. The protoscolex that develops into the adult form in the definitive host is enveloped by a complex cellular syncytial tegument, where all metabolic interchange takes place. Little information is available as to the electrical activity of the parasite in this developmental stage. To gain insight into the electrical activity of the parasite at the larval stage, here we conducted microelectrode impalements of bovine lung protoscoleces (PSCs) of *Echinococcus granulosus* in normal saline solution. We observed two distinct intra-parasitic potentials, a transient peak potential and a stable second potential, most likely representing tegumental and intra-parasitic extracellular space electrical potential differences, respectively. These values changed upon the developmental status of the parasite, its anatomical regions, or time course after harvesting. Changes in electrical potential differences of the parasite provide an accessible and useful parameter for the study of transport mechanisms and potential targets for the development of novel antiparasitic therapeutics.

Author summary

Hydatid disease is a parasite-caused zoonosis that causes high morbidity and mortality and has a great impact on public health. The disease has no known cure, and the main lines of treatment include surgery and medical treatments which are not satisfactory, so new drug compounds are urgently needed. Genome sequencing of the parasite has identified different genes encoding ion channels in *Echinococcus granulosus*, making ion channel inhibitors a promising target for treating hydatidosis. However, no easy

technical approaches are available to test the electrical contribution of ion channels to parasite physiology. In the present study, we used the microelectrode impalement technique to determine the electrical properties of the larval stages of the parasite harvested from infected cow lungs. We observed transient electrical potentials not previously reported for the parasite, and changes in these parameters associated with its developmental stage and aging. Our findings indicate that microelectrode impalement of protoscoleces of *Echinococcus granulosus* may be a strategy of choice to explore and test possible drugs suggested for their therapeutic potential against hydatid disease. Further evaluation of parasites coming from other animals and humans may help address important issues in the treatment and prevention of the hydatid disease.

Introduction

Cystic echinococcosis or hydatidosis encompasses a group of important zoonotic diseases caused by the metacestode (larval stage) of Taenia tapeworms belonging to the genus *Echinococcus*. The disease is mainly transmitted in livestock-raising areas, and the two most important zoonotic species of this genus are *E. granulosus* and *E. multilocularis*, causing cystic -or unilocular- echinococcosis (CE) and alveolar -or multivesicular- echinococcosis (AE), respectively [1, 2]. *E. granulosus* is the most widespread, with endemic foci in various continents, including South America, the entire Mediterranean littoral, central Asia, China, Australia, and Africa. In South America, CE is endemic in Argentina, Uruguay, Brazil, Chile, and some regions of Perú and Bolivia [3]. In Argentina, this zoonosis spreads through genetically distinct populations of the parasite [4].

E. granulosus undergoes a developmental cycle where sexual development of the adult stage occurs in the small intestine of dogs. Excreted eggs (larval stage) undergo

69 embryonic development into oncospheres that scatter to the environment by fecal
70 deposition. The cycle continues after ingestion of oncospheres by intermediate hosts,
71 including humans. The embryos that hatch from the eggs penetrate the intestinal mucosa
72 and distribute to the liver or other organs, undergoing metamorphosis into the next
73 larval stage, the metacestode [3]. Closing the life-cycle, the metacestode is eventually
74 ingested by a definitive host (mostly dog) to develop into a segmented and sexually
75 mature adult stage again [5].
76 Metacestodes constitute fluid-filled cysts with an inner thin germinal layer where large
77 numbers of protoscoleces (PSCs) are formed by asexual multiplication. The germinal
78 layer invaginates to form vesicles and brood capsules [6]. PSCs remain invaginated
79 within the mucopolysaccharide-coated basal region of the protoscoleces tegument
80 (invaginated PSC) to protect the scolex until evagination in the definitive host
81 (evaginated PSC). The precise stimulation for parasite evagination remains unknown,
82 but environmental changes such as variations in temperature and osmotic pressure may
83 be among the determining factors [6, 7].
84 Like other cestodes, *E. granulosus* lacks a digestive system, such that the parasite
85 absorbs water, salts, and nutrients through the external tegument [8]. Thus, the study of
86 the functional properties of the syncytial tegument is necessary for understanding host-
87 parasite interactions. However, little information is available about the physiological
88 differences between the invagination/evagination processes in protoscoleces (PSCs) of
89 *E. granulosus*. Electrophysiological techniques are useful in the assessment of the
90 electrical properties of PSCs and can help in the understanding of electrolyte transport
91 by the tegumental epithelium. Microelectrode recordings have previously been used to
92 characterize tegumental potential differences (PD) of *Schistosoma mansoni* [9] and the
93 tegumental potential differences (PD) of ovine strain *E. granulosus* [8], where

significant changes were observed upon immunological and chemical manipulations [10, 11].

Here we used microelectrode recordings from PSCs of *E. granulosus* from lungs of bovine origin to obtain parasitic potential differences (PD). Two distinct parasitic PD, transient and stable trans-tegumental PD, were recorded from both invaginated and evaginated PSCs. Data provide, to our knowledge, the first evidence for electrical potential differences from bovine strain *E. granulosus* that showed significant differences with previously reported *E. granulosus* from the ovine strain [8]. These results may help understand the molecular mechanisms associated with ion transport and hydroelectrolytic balance into the parasite.

Materials & Methods

Parasites

Protoscoleces of *Echinococcus granulosus* were obtained from hydatid cysts of naturally infected cattle lungs from a local abattoir. The parasites were collected and washed as originally described [12] and resuspended in PBS (pH 7.4) supplemented with penicillin (100 units/ml), streptomycin (100 µg/ml), and amphotericin (0.25 µg/ml). The PSCs were kept at 4°C and used up to one month after harvesting. Viability was evaluated based on both the methylene blue exclusion method and microscope examination (10X) of body movements.

Saline solutions

PSCs were incubated in Ringer Krebs Solution (RKS) containing 121 mM NaCl, 5 mM KCl, 22.5 mM $MgCl_2$, 2.5 mM $CaCl_2$, 10 mM Hepes and 5.6 mM glucose, pH 7.4. All other constituents, osmolarity, and pH were preserved.

In vitro incubation procedures

Parasites were stored at 4°C in PBS (supplemented with antibiotics and antimycotics) and immediately before the impalement, PSCs were washed and preincubated for 2 h at 37°C in fresh RKS without antibiotics.

Electrophysiology

Electrical recordings were conducted with a single microelectrode high input impedance (>10^{11} Ω) amplifier-intracellular electrometer (Model IE-210, Warner Instruments, Hamden, CT) with an internal 4-Pole low-pass Bessel filter set at 20 kHz and sampling rate at 10 kHz. The electrometer was connected in parallel to an Analog-Digital Converter (TL-1 interface. Tecmar, Solon, OH) that fed the digital input of a personal computer running Axograph (Axon Instruments, Union City, CA, USA) as a digital oscilloscope.

Microelectrode recordings

Microelectrodes from glass capillaries (Biocap, Buenos Aires, Argentina) with 1.25 mm internal diameter were pulled on a PB-7 pipette puller and heat-polished on an MF-9 pipette polisher (Narishige, Tokyo, Japan), and filled with filtered 3 M KCl solution. Tip resistance ranged between 10 and 40 MΩ. The reference electrode was a wider tip glass capillary, also filled with 3 M KCl solution, connected to Cl^--plated silver wire

(Ag/AgCl) and to the ground socket of the electrometer. The recording chamber consisted of a glass slide where an aliquot (500 µl) of a protoscolex suspension was added (~100 PSCs/ml). Parasites were impaled after being individually captured and held with a suction micropipette (Fig. 1c). Impalements were performed under optical microscopy with an IMT2 Olympus inverted microscope (x10). All impalements were performed at room temperature after PSC incubation at 37°C. The criteria for acceptable impalement included: (1) a sharp deflection to a peak potential after electrode penetration into the PSC; and (2) an abrupt return to the original baseline (0 mV) after removal from the parasite.

Data analyses

Data analysis was conducted with Clampfit 10.7 (Axon Instruments). Sigmaplot 11.0 (Jandel Scientific, Corte Madera, CA) was used for statistical analysis and graphics. Unless otherwise indicated, only values from animals up to 6 days post-harvest were considered for statistical analyses due to significant changes in tegumental voltages afterward. Normal distributions of data were examined using the Shapiro-Wilk W test for normality where $p < 0.05$ indicated a significant departure from normality. Upon failure of the Shapiro-Wilk W test, the Box-Cox normality plot was performed to transform data for normalization [13]. Correlation between potential differences (PD) was performed by the linear regression model, testing the resultant equation against the null hypothesis of a slope equal to zero, considering a $p < 0.05$. Student t-test and one-way ANOVA were used to determine statistical significance between different experimental groups. Averages of corrected data values were expressed as the mean ± SEM for each experimental condition per number of (n) or per number of PSCs (N).

Results

Microelectrode recordings of protoscoleces

The electrical behavior of bovine lung PSCs was explored by microelectrode impalement as previously reported for *Schistosoma mansoni* [9, 14-16] and PSCs of *E. granulosus* of ovine origin [8]. Both invaginated and spontaneously evaginated PSCs were impaled. Upon microelectrode penetration of the **tegumental surface (Fig. 1c) a rapid negative transient deflection in electrical potential was always recorded (*n* = 135, Fig. 1D), which we referred to as "peak" or potential difference 1 (*PD_1*).**

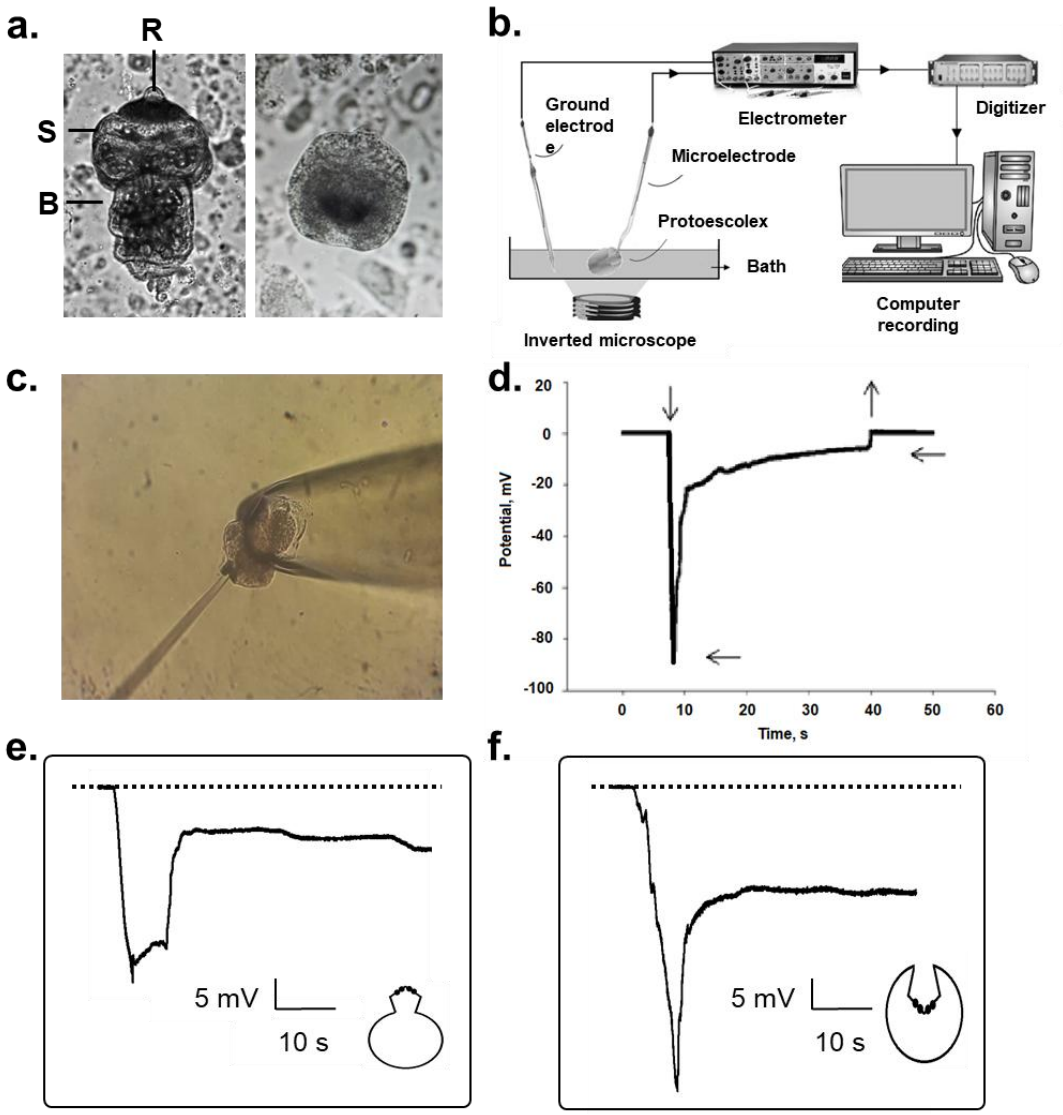

Fig. 1: Electrical microelectrode recordings of PSCs from *E. granulosus*. (**a)** Left: Evaginated PSC; **R**= Rostellum, **S**= Sucker, **B**= Body; Right: Invaginated PSC. **(b)** Electrical setup. Both ground and impaling microelectrodes were connected to an electrometer and recorded through an A/D system to a personal computer. **(c)** Evaginated PSC held by a suction pipette and impaled with a recording microelectrode (shown on Left). **(d)** Representative recording of an invaginated PSC shows deflections upon impalement (downward vertical arrow) and withdrawal (upward vertical arrow). A typical tracing shows transient (peak, PD_1) and more stable lower (plateau, PD_2) potentials. Horizontal arrows indicate recorded values for PD_1 and PD_2, respectively. **(e)** Example of the tegumental potential of invaginated PSC. **(f)** Example of the tegumental potential of evaginated PSC. Dashed lines represent 0 mV. Please note that no upward deflections after withdrawal of microelectrode are indicated.

This transient potential always spontaneously decayed to another lower, referred to as "plateau" potential (PD_2), even when the microelectrode was not advanced more deeply into the parasite. Both PD_1 and PD_2 were always discernible and observed in either invaginated or evaginated parasites. Although impalements for either invaginated or evaginated PSCs were always conducted under similar conditions, raw values did not follow a Normal distribution (Fig. 2). Thus, group values (either invaginated or evaginated PSCs) were transformed by the Box-Cox algorithm [13], to allow quantitative comparisons. Relative to the bath (0 mV), the PD_1 values for invaginated PSCs ranged between -179.4 and -14.4 mV with a mean of -64.8 ± 1.4 mV (n = 49). The PD_2 values for the same group ranged from -88.4 to -6 mV, with a mean value of -23.2 ± 0.3 mV (n = 49), thus representing a ΔPD ($PD_1 - PD_2$) of -41.6 mV (Table 1). Evaginated parasites instead, had PD_1 values that ranged from -231.3 to -20.7 mV with a mean of -92.9 ± 0.5 mV (n = 86). These potentials shifted to a PD_2 value that ranged between -77.5 mV and -23.6 mV, with a mean value of -33.5 ± 1.8 mV (n = 86), representing a ΔPD ($PD_1 - PD_2$) of -59.4 mV (Table 1). Thus, mean PD_1 and PD_2 values were statistically different among groups, indicating different tegumental

electrical properties ($p \leq 0.05$; Table 1). The ΔPD values were also statistically different among groups (Table 1), being more negative in the evaginated state ($p < 0.0001$).

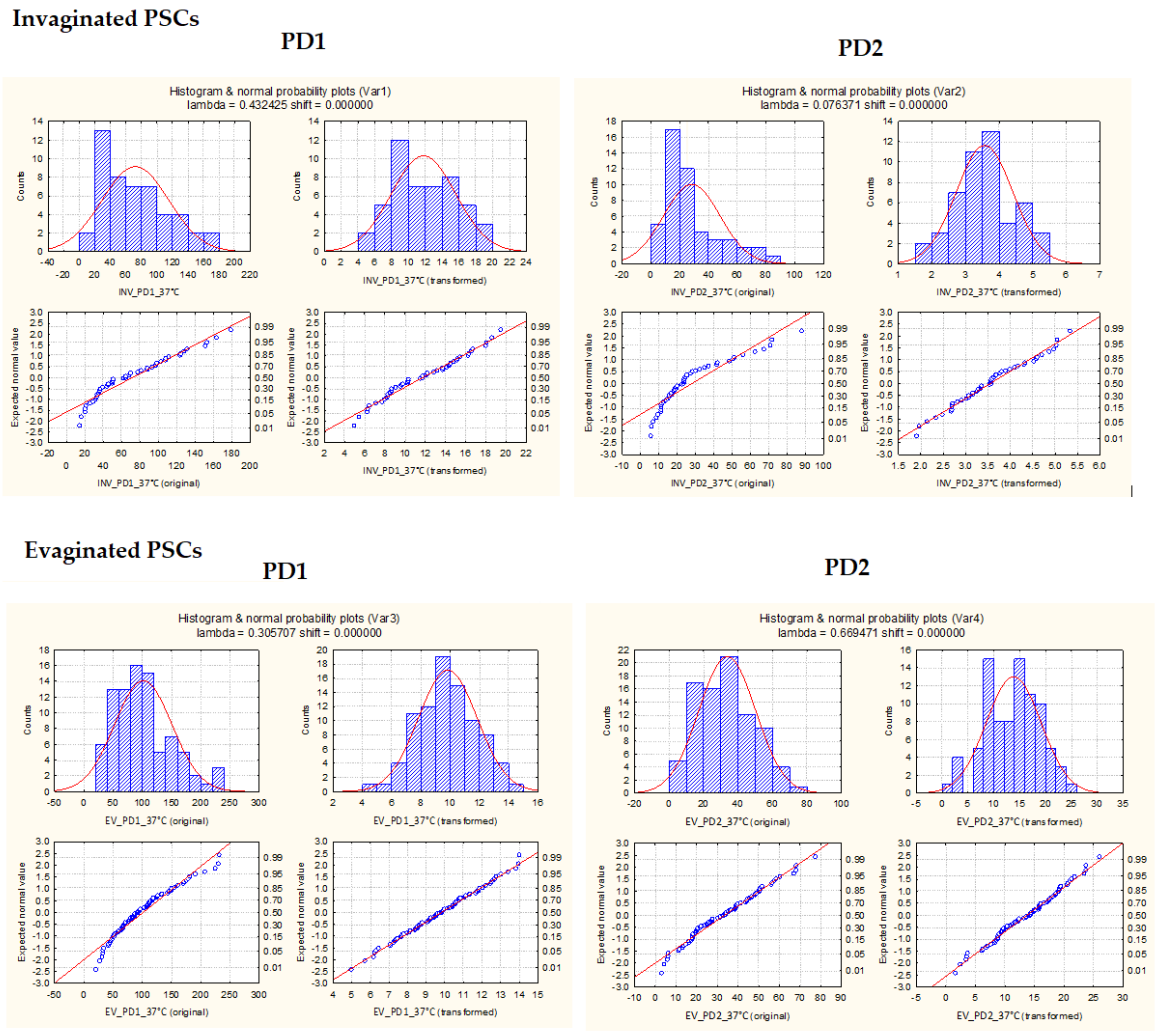

Fig. 2: Tegumental potential data distributions. Recordings of PSCs from *E. granulosus*. Left panels indicate PD_1 values and right panels PD2 values, for invaginated (Top panels, n = 49 values) and evaginated PSCs (Bottom panels, n = 86 values), respectively. Values (mV) are expressed as the mean ± SEM for peak (PD_1) and plateau (PD_2), respectively.

Table 1. Tegumental potentials of PSCs from *E. granulosus*.

Dev stage	***PD_1***	***PD_2***	***ΔPD***	***p value***
Invaginated	-64.8 ± 1.4 (n = 49)	-23.2 ± 0.3 (n = 49)	41.6	< 0.001
Evaginated	-92.9 ± 0.5 (n = 86)	-33.5 ± 1.8 (n = 86)	59.4	< 0.001

To explore whether impaling itself modified the PD values by either tissue damage or KCl leakage from the pipette, multiple sequential measurements (five events/organism) were also conducted in individual PSCs. For invaginated PSCs, mean PD_1 values were -79.3 mV ± 11.5 (N = 15) that decayed to a mean PD_2 value of -32.6 mV ± 4.9 (N = 15). For evaginated PSCs, PD_1 was -93.1 mV ± 14.3 (N = 30) that decayed to a PD_2 value of -35.3 mV ± 7.2 (N = 30). Thus, mean individual values did not differ significantly from those obtained from a large number of individual measurements ($p > 0.05$; Table 1), and therefore impalement itself did not contribute to the transient peaks (PD_1), nor affected the ΔPD values observed in either developmental stage of the parasite.

Time response of the impalements

Because of the different enfolding in the tegumental epithelium between the invaginated and evaginated parasites, the time taken for full peak polarization after impalement was also compared between groups. Depolarizations lasted between 100 and 1000 milliseconds, with slopes of -3.7 ± 0.02 mV/sec (n = 8), and -10.3 ± 0.13 mV/sec (n = 5) for invaginated and evaginated PSCs, respectively. Thus, the change in potential at impalement was three times faster in evaginated PSCs ($p < 0.001$). The PD_1 and PD_2 potentials were well defined and statistically different within and among groups, as determined in both invaginated and evaginated PSCs ($p < 0.001$, Table 1). However, microelectrode recordings were statistically higher in evaginated PSCs than invaginated PSCs, representing a ΔPD_1 of almost 30 mV, and ΔPD_2 of only 10 mV ($p < 0.05$, Table 1). To explore whether the developmental stage of evagination affected this interaction, the correlation between PD_1 and PD_2 was also determined in either stage (Fig. 3c and 3d). A statistically significant correlation was observed between the magnitude of the tegumental and intra-parasitic potentials ($r > 0.5$), with a slope of 0.199 ± 0.029 (n = 49)

and 0.266 ± 0.054 (n = 86) for invaginated and evaginated PSCs, respectively. However, the correlations were not significantly different among groups, suggesting electrical continuity between the functional compartments in both invaginated and evaginated PSCs.

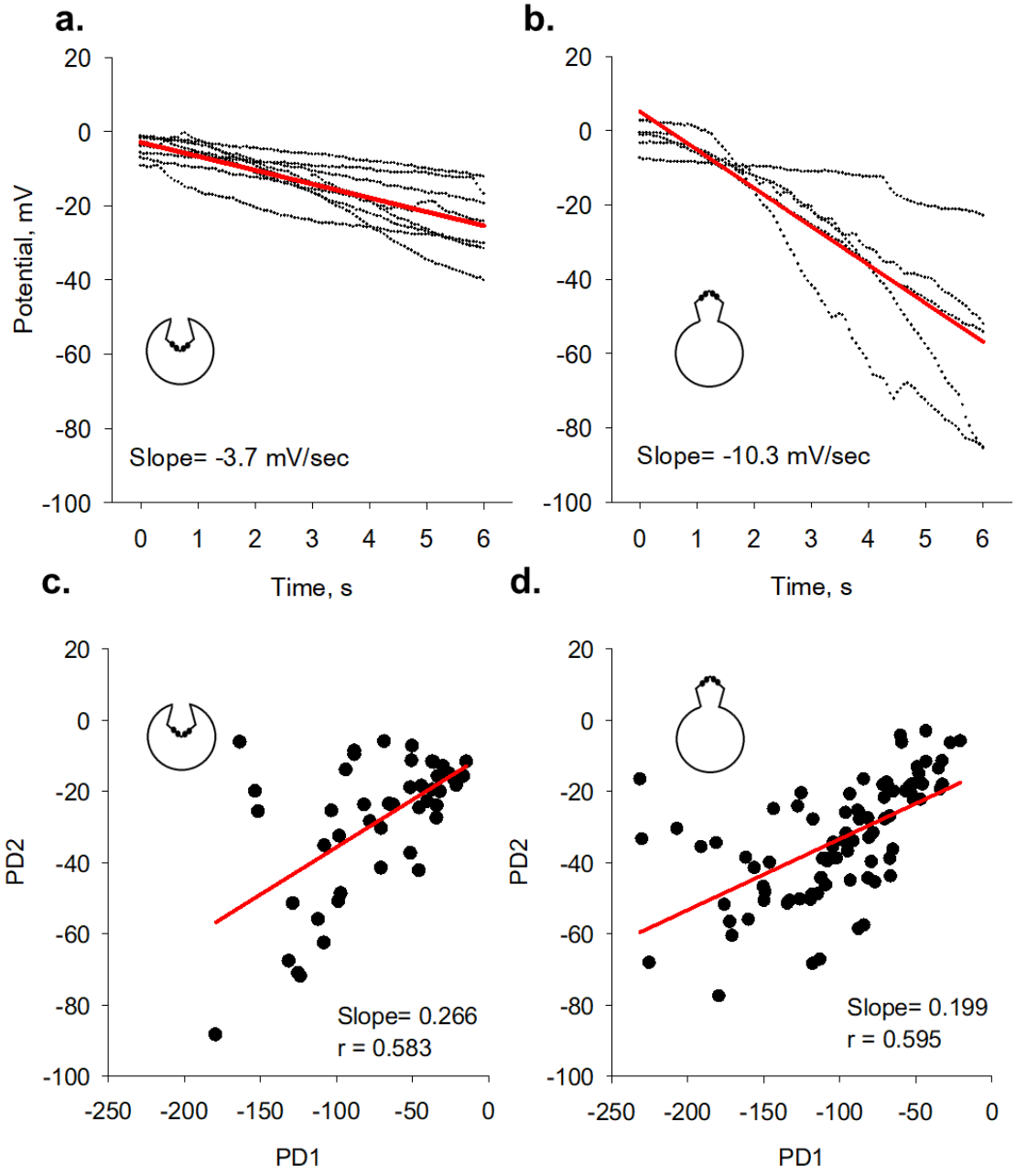

Fig. 3: Time-course of impalement and correlations between PD_1 and PD_2. Impalements were carried out at 37°C in RKS, for both invaginated and evaginated PSCs (Left and Right panels, respectively). Solid red lines indicate the best linear fitting of time deflections (shown as dotted lines) under each

condition. Plots **(a)** & **(b)** show slopes in mV/sec as shown at bottom. Plots **(c)** & **(d)** show the correlation between PD_1 (mV) and PD_2 (mV), for invaginated and evaginated PSCs, respectively.

Effect of aging on the tegumental potentials

Electrical recordings varied through time post-harvesting and decreased significantly after the sixth day for invaginated PSCs and after the twelfth day for evaginated PSCs (Fig. 4). Therefore, mean values were considered from measurements conducted up to a week after collection from hydatid cysts.

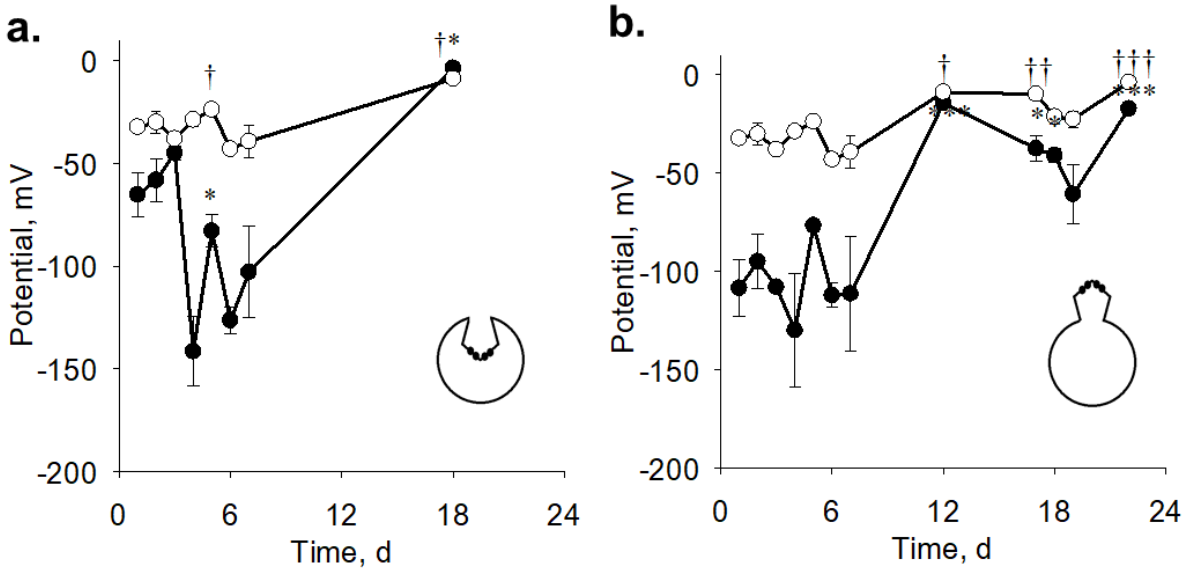

Fig. 4. Effect of aging on the electrical potentials of PSCs from *E. granulosus*. Graphs show parasitic potentials at different times post-harvest in days (d) from invaginated **(a)** and evaginated PSCs **(b)**, respectively. Filled symbols correspond to PD_1 and open symbols to PD_2. Values are the mean ± SEM, for *n* between 3 and 56. Symbols † or * indicate statistically significant difference from day 1 (PSCs harvesting) for PD_1 or PD_2 respectively, with †$p < 0.05$, ††$p < 0.01$, †††$p < 0.001$ and *$p < 0.05$, ***$p < 0.001$.

Parasitic potentials in identified anatomical regions of evaginated PSCs

While invaginated PSCs may be expected to represent a single parasitic compartment, evaginated parasites may offer distinct and well-defined anatomical regions [17, 18]. Because similar correlations were observed between PD_1 and PD_2 in both populations (Fig. 3c and 3d) we also explored whether the process of evagination exposed a particular electrical compartment not defined in the invaginated state. For this, recordings were obtained from the three identifiable anatomical regions of evaginated PSCs [17, 18] including the rostellum, the sucker, and body regions of the parasite (Fig. 1a). PD_1 and PD_2 remained different among regions, with ΔPD in the 36.8 to 50.7 mV range (Table 2). The trans-tegumental potential (PD_1) obtained from the rostellum was significantly higher than that from either the neck or body of the evaginated PSC (Table 2). Even, intra-parasitic potential (PD_2) showed significant statistical differences among the three anatomical regions, suggesting the distinct compartmental distribution of potential throughout the parasite.

Table 2. Tegumental potentials from different anatomical regions of evaginated PSCs.

	n	*PD1*	*PD2*	ΔPD	*p value*
Rostellum	20	-81.5 ± 1.4[a]	-30.8 ± 0.8[a]	50.7	< 0.001
Sucker	64	-65.9 ± 2.2[b]	-27.4 ± 0.7[b]	38.5	< 0.001
Body	42	-60.4 ± 1.8[b]	-23.6 ± 0.7[c]	36.8	< 0.001

Mean ± SEM followed by the same letter in each column were not significantly different from each other (Tukey's test, $p < 0.01$).

Discussion

The present study provides, to our knowledge, the first reported characterization of the tegumental electrical properties of PSCs of *Echinococcus granulosus* from bovine lung. The values and electrical features were different from those reported for PSCs of

297 *Echinococcus granulosus* from the ovine strain [8] and interestingly were more similar
298 to those of *Schistosoma mansoni* [9]. We observed that upon penetration of the
299 tegumental surface of the PSC, the first peak of negative potential (PD_1) was recorded
300 that was lower in invaginated PSCs as compared to evaginated PSCs. The PD_1 values
301 were independent of the duration or depth of the impalement, and spontaneously
302 decayed to a lower plateau value (PD_2), which remained stable and, in all cases was
303 lower in invaginated PSCs.
304 Because the syncytial tegument of *E. granulosus* is very thin, 2 to 3 µm wide [19], and
305 despite the actual location of the impaled microelectrode was not ascertained, the first
306 peak voltage deflection (PD_1) should correspond to the trans-tegumental potential, in
307 agreement with previous reports of ovine PSCs of *E. granulosus* [8], and *Schistosoma*
308 *mansoni* [9, 20]. Elimination of the tegument by addition of either deoxycholate or
309 Triton X-100 always elicited a rapid and irreversible depolarization of this particular
310 electrical potential difference. Moreover, it was demonstrated by iontophoretic injection
311 of horseradish peroxidase into *S. mansoni* that PD_1 originated in the tegumental
312 epithelium [20]. The second potential observed in that study, which is similar to PD_2
313 obtained in the present report, was ascribed to muscle masses below the tegumental
314 membrane [9, 20]. This is also in agreement with electrophysiological studies
315 describing the degree of electrical coupling between tegument and muscle of *S.*
316 *mansoni*, were presented by Thompson et al [16].
317 Aging is another parameter that may bring information regarding the location of PD_1
318 and PD_2. Ibarra and Reisin [8] reported that under control conditions, *E. granulosus*
319 PSCs from ovine origin remained stable up to 25 days. However, the present study on
320 PSCs from bovine lung origin showed a significant decrease in PD_1 after 6 days post-

harvest, as compared to PD_2. On the other hand, no invaginated PSCs could be found after 20 days post-harvest, because gradual development into the evaginated stage.

The reason(s) for the differences between the shape and magnitude of the PDs in ours and Ibarra and Reisin [8] could span from technical details of the electrical recordings to the origin and species of the PSCs, including the *E. granulosus* genotypes. Further experimentation will be required to ascertain the nature of these changes.

The present study indicates that although the general properties of the syncytial tegument may remain the same in different developmental stages of the parasite, the speed of depolarization at impalement and PD_1 and PD_2 values were statistically higher in the evaginated stage as compared to the invaginated stage of the parasite. Thus, it is possible that the invaginated parasite could provide a second electrical barrier that is eliminated upon evagination. However, the magnitude of PD_1 and PD_2 were similarly correlated in both developmental stages, an indication that the electrical compartments remained identically coupled.

Previous studies have not reported on the tegumental potentials of the evaginated stage of the PSC from *Echinococcus granulosus*. The electrical data of the anatomical regions of the evaginated parasite obtained in the present study further suggest that different parts may provide specific contributions to the invaginated stage, where the anatomical regions such as the rostellum and the neck are intra-parasitic. Moreover, different tegumental potentials have been reported in anatomical regions of *Schistosoma* [16].

Little is known as to the electrodiffusional pathways that contribute to the electrical potential differences in *Echinococcus* and other flatworms. Cantiello, Ibarra & Reisin [21] observed that the passive K^+ influx corresponded to a simple diffusional mechanism distributed in at least two compartments, one small and faster and the other large and slower ionic exchange, although no anatomical correlates of the parasite were

reported. The ion channel species responsible for these movements have yet to be identified, as well as their contribution to the electrophysiology of the parasite. Grosman and Reisin provided preliminary evidence for the presence of cation-selective channels in extracted membranes of *E. granulosus* PSCs from ovine origin [22, 23]. The recent genomic sequencing of *E. granulosus* and other cestodes [6, 24] may help identify the molecular fingerprints of the channel and transporter species, and assess their relevance as possible pharmacological targets [25]. To date, useful antiparasitic drugs include potential Ca^{2+} channel blockers such as praziquantel [26, 27], and benzimidazoles, such as mebendazole and albendazole, that modify the microtubular cytoskeleton [28]. New ion channel targets and relevant interactions could be expected to bring about novel therapeutic strategies [29-31]. We recently obtained preliminary information to suggest that known links between excitable cation channels and the actin cytoskeleton [32] may help potentiate the ability of praziquantel to paralyze the *Echinococcus granulosus* PSCs [33].

In summary, the present study provides evidence that PSCs of *Echinococcus granulosus* from the bovine strain present complex tegumental potentials remarkably differ from those previously reported for a similar preparation from sheep origin. Two distinct functional compartments were identified of tegumental origin and extracellular domain of the intra-parasitic milieu, respectively. Future studies will be required to assess the nature of the differences, genetic or otherwise from those reported with ovine *E. granulosus*, and those expected from other intermediary species. The microelectrode measurements of parasitic potentials may prove an invaluable tool in helping characterize the contribution of various ion channel species and enzymatic transporters in cestodes, and also provide a rapid testing approach to explore and identify new pharmacological targets.

Acknowledgments

The authors wish to acknowledge the National Research Council of Argentina (CONICET) for funding of the present study (PUE 2292180100054CO).

Author Contributions

Conceptualization: Horacio F. Cantiello

Data curation: Mónica P. A. Carabajal, Marcos A. Durán, Santiago Olivera

Resources: Santiago Olivera, María José Fernández Salom

Formal analysis: Mónica P. A. Carabajal, Horacio F. Cantiello

Funding acquisition: Horacio F. Cantiello

Supervision: Horacio F. Cantiello

Investigation: Horacio F. Cantiello, Mónica P. A. Carabajal, Marcos A. Durán, Santiago Olivera, María José Fernández Salom

Writing – original draft: Horacio F. Cantiello, Mónica P. A. Carabajal

Writing – review & editing: Horacio F. Cantiello

References

1. Eckert J, Deplazes P. Biological, epidemiological, and clinical aspects of echinococcosis, a zoonosis of increasing concern. Clin Microbiol Rev. 2004; 17(1):107-35. https://doi.org/10.1128/CMR.17.1.107-135.2004 PMID: 14726458

2. Thompson R, Lymbery A. The nature, extent and significance of variation within the genus *Echinococcus*. Adv Parasitol. 1988;27:209-58. https://doi.org/10.1016/S0065-308X(08)60356-5

3. Moro P, Schantz PM. Echinococcosis: a review. Intl J Infect Dis. 2009;13(2):125-33. https://doi.org/10.1016/j.ijid.2008.03.037

4. Kamenetzky L, Gutierrez AM, Canova SG, Haag KL, Guarnera EA, Parra A, et al. Several strains of *Echinococcus granulosus* infect livestock and humans in Argentina. Infect Genet Evol. 2002;2(2):129-36. https://doi.org/10.1016/S1567-1348(02)00131-4

5. Camargo de Lima J, Monteiro KM, Basika Cabrera TN, Paludo GP, Moura H, Barr JR, et al. Comparative proteomics of the larval and adult stages of the model cestode parasite *Mesocestoides corti*. J Proteom. 2018;175:127-35. https://doi.org/10.1016/j.jprot.2017.12.022

6. Koziol U, Brehm K. Recent advances in *Echinococcus genomics* and stem cell research. Vet Parasitol. 2015;213(3-4):92-102. https://doi.org/10.1016/j.vetpar.2015.07.031

7. Thompson R. Chapter Two - Biology and Systematics of Echinococcus. In: Thompson RCA DP, Lymbery AJ (Eds.), editor. Advances in Parasitology Academic Press; 2017. p. 65-109. https://doi.org/10.1016/bs.apar.2016.07.001

8. Ibarra C, Reisin IL. *Echinococcus granulosus*: Characterization of the electrical potential of the syncytial tegument of protoscoleces incubated *in vitro*-effect of inhibitors. Exp Parasitol. 1994;78(4):400-9. https://doi.org/10.1006/expr.1994.1044

9. Fetterer R, Pax R, Bennett J. *Schistosoma mansoni:* Characterization of the electrical potential from the tegument of adult males. Exp Parasitol. 1980;49(3):353-65. https://doi.org/10.1016/0014-4894(80)90071-5

10. Reisin IL IC, Cybel B, Rotunno CA, Cantiello HF. Mecanismos de acción del mebendazol sobre el *Echinococcus granulosus* en su estadío larval estudiado *in vitro*.

419 Bases para la interpretación de los resultados de la quimioterapia experimental y clínica
420 Arch Intl Hidatidosis XXVIII. 1988:442-70.
421 11. Ferreira A, Trecu T, Reisin I. *Echinococcus granulosus*: study of the *in vitro*
422 complement activation by protoscoleces by measuring the electric potential difference
423 across the tegumental membrane. Exp parasitol. 1992;75(3):259-68.
424 https://doi.org/10.1016/0014-4894(92)90211-R
425 12. Reisin I, Rabito C, Cantiello H. Water and electrolyte balance in protoscoleces
426 of *Echinococcus granulosus* incubated *in vitro*: Effect of metabolic inhibitors. Intl J
427 Parasitol. 1981;11(5):405-10. https://doi.org/10.1016/0020-7519(81)90013-8
428 13. Box G, Cox D. An analysis of transformation. J Royal Stat Soc, Series B
429 (Methodological). 1964;26(2):211-52.
430 https://doi.org/10.1111/j.25176161.1964.tb00553.x
431 14. Fetterer RH, Pax RA, Bennett JL. *Schistosoma mansoni*: Direct method for
432 simultaneous recording of electrical and motor activity. Exp Parasitol. 1977;43(1):286-
433 94. https://doi.org/10.1016/0014-4894(77)90033-9
434 15. Fetterer R, Pax R, Bennett J. Na^+–K^+ transport, motility and tegumental
435 membrane potential in adult male *Schistosoma mansoni*. Parasitology. 1981;82(1):97-
436 109. https://doi.org/10.1017/S0031182000041895
437 16. Thompson D, Pax R, Bennett J. Microelectrode studies of the tegument and sub-
438 tegumental compartments of male *Schistosoma mansoni*: an analysis of
439 electrophysiological properties. Parasitology. 1982;85(1):163-78.
440 https://doi.org/10.1017/S0031182000054238
441 17. Martínez C, Paredes R, Stock R, Saralegui A, Andreu M, Cabezón C, et al.
442 Cellular organization and appearance of differentiated structures in developing stages of

443 the parasitic platyhelminth *Echinococcus granulosus*. J Cell Biochem. 2005;94(2):327-
444 35. https://doi.org/10.1002/jcb.20294

445 18. Galindo M, Schadebrodt G, Galanti N. *Echinococcus granulosus*: cellular
446 territories and morphological regions in mature protoscoleces. Exp Parasitol.
447 2008;119(4):524-33. https://doi.org/10.1016/j.exppara.2008.04.013

448 19. Morseth DJ. Fine structure of the hydatid cyst and protoscolex of *Echinococcus*
449 *granulosus*. J Parasitol. 1967;53:312-25. https://doi.org/10.2307/3276582

450 20. Bricker CS, Pax R, Bennett J. Microelectrode studies of the tegument and sub-
451 tegumental compartments of male *Schistosoma mansoni*: anatomical location of sources
452 of electrical potentials. Parasitology. 1982;85(1):149-61.
453 https://doi.org/10.1017/S0031182000054226

454 21. Cantiello H, Ibarra C, Reisin I. Flujos de K^+ y potenciales eléctricos a través de
455 las membrana de *Echinococcus granulosus* incubado "*in vitro*". IX Reunión Anual de la
456 Sociedad Argentina de Biofísica; Bermejo, Mendoza.1980.

457 22. Grosman C, Reisin IL. *Echinococcus granulosus*: partial characterization of the
458 conductive properties of two cation channels from protoscoleces of the ovine strain,
459 reconstituted on planar lipid bilayers. Exp Parasitol. 1995;81(4):546-55.
460 https://doi.org/10.1006/expr.1995.1148

461 23. Grosman C, Reisin I. Interconverting gating modes of a nonselective cation
462 channel from the tapeworm *Echinococcus granulosus* reconstituted on planar lipid
463 bilayers. J. Membrane Biol. 1997;158(1):87-94. https://doi.org/10.1007/s002329900246

464 24. Tsai IJ, Zarowiecki M, Holroyd N, Garciarrubio A, Sanchez-Flores A, Brooks
465 KL, et al. The genomes of four tapeworm species reveal adaptations to parasitism.
466 Nature. 2013;496(7443):57-63. https://doi.org/10.1038/nature12031

467 25. Nor B, Young ND, Korhonen PK, Hall RS, Tan P, Lonie A, et al. Pipeline for
468 the identification and classification of ion channels in parasitic flatworms. Parasites
469 Vectors. 2016;9(1):1-12. https://doi.org/10.1186/s13071-016-1428-2
470 26. Doenhoff MJ, Cioli D, Utzinger J. Praziquantel: mechanisms of action,
471 resistance and new derivatives for schistosomiasis. Curr Opin Infect Dis.
472 2008;21(6):659-67. https://doi.org/10.1097/QCO.0b013e328318978f
473 27. Wu W, Wang W, Huang Y-x. New insight into praziquantel against various
474 developmental stages of *schistosomes*. Parasitol Res. 2011;109(6):1501-7.
475 https://doi.org/10.1007/s00436-011-2670-3
476 28. Lacey E. Mode of action of benzimidazoles. Parasitol Today. 1990;6(4):112-5.
477 https://doi.org/10.1016/0169-4758(90)90227-U
478 29. Prole DL, Taylor CW. Identification of intracellular and plasma membrane
479 calcium channel homologues in pathogenic parasites. PloS ONE. 2011;6(10):e26218.
480 https://doi.org/10.1371/journal.pone.0026218
481 30. Jimenez V, Docampo R. Molecular and electrophysiological characterization of
482 a novel cation channel of *Trypanosoma cruzi*. PLoS Pathog. 2012;8(6):e1002750.
483 https://doi.org/10.1371/journal.ppat.1002750
484 31. Greenberg RM. Ion channels and drug transporters as targets for anthelmintics.
485 Curr Clin Micro Rpt. 2014;1(3-4):51-60. https://doi.org/10.1007/s40588-014-0007-6
486 32. Lader AS, Kwiatkowski DJ, Cantiello HF. Role of gelsolin in the actin filament
487 regulation of cardiac L-type calcium channels. Am J Physiol. 1999;277(6):C1277-C83.
488 https://doi.org/10.1152/ajpcell.1999.277.6.C1277
489 33. Durán MA, Olivera SR, Cantiello HF. Increase in pharmacological potency of
490 Praziquantel by cytoskeletal modifiers in protoscoleces of *Echinococcus granulosus*.
491 XXXIII Jornadas Nacionales de Hidatidosis; Octubre 6; Catamarca, Argentina, 2018.